Comparative Study on Fractional Isothermal Chemical Model

Khaled M. Saad[a,b]

[a]Department of Mathematics, College of Arts and Sciences ,
Najran University, Najran, Kingdom of Saudi Arabia

[b]Department of Mathematics, Faculty of Applied Science,
Taiz University, Taiz, Yemen

E-Mail khaledma_sd@hotmail.com

Abstract

This article investigates a family of approximate solutions for the fractional isothermal chemical (FIC) equation based on mass action kinetics for autocatalytic feedback, involving the conversion of a reactant in the Liouville-Caputo sense. We apply two methods to construct numerical solutions of the FIC equation. By the first method, the spectral collocation method (SCM), we reduce the FIC equation to a system of algebraic equations using Chebyshev polynomials of the third kind (CPTK). We then use the Newton-Raphson method (NRM) to solve the system of algebraic equations. By the second method, using properties of Lagrange polynomial interpolation (LPI) after applying the fundamental theorem of fractional calculus, we evaluate numerical solutions of the FIC equation. We compare these numerical solutions and compute the absolute error for varying parameter values. The results confirm the efficiency of the methods and their computationally favorable use for the numerical treatment of the model equations.

2020 Mathematics Subject Classification: 34A08; 35A22; 41A30; 65N22.

Key Words: Fractional derivatives; fractional isothermal chemical; Chebyshev polynomials of the third-kind; Chebyshev spectral collocation method;Lagrange polynomial interpolation; Newton-Raphson method.

1. Introduction, Definitions and Preliminaries

Many real world problems cannot be modeled using equations with standard derivatives. So many researchers have then been attracted to problems governed by fractional derivatives. Fractional differential equations can be used and applied to model many applications, as they have proven to be effective for theoretical work and in simulations. Fractional-order equations govern systems arising in electrical, electronic, mechanical, biological and other application areas and are represented either through transfer functions or state space. Fractional equations are based on the use of fractional calculus to describe and model such systems, as well as in a range of control and physical applications. The use of fractional calculus can improve and generalize well established control methods and strategies, for more details see [1, 2]. Unfortunately, for most of these models it is difficult to find an exact solution. Therefore, many researchers have

been interested in deriving approximate and numerical methods to find approximate and numerical solutions of these models, which allows the study of the dynamics and behavior of the systems governed by these models. There are many such methods, including homotopy analysis [3, 4], He's variational iteration method [5, 6], Adomian's decomposition method [7, 8], Fourier spectral methods [9], finite difference schemes [10] and collocation methods [11]. Recently, numerical and approximate methods have been used to find numerical solutions and study the dynamical behavior of many fractional systems. Devendr et al [15] studied exothermic reactions with a constant heat source in a porous medium with strong memory effects. They used the fractional Laplace decomposition technique to find numerical solutions. Devendr et al [13] investigated the fractional extension of the vibration equation for very large membranes, which has several distinct special cases in the Atangana-Baleanu sense. Dumitru et al [14] investigated a harmonic oscillator with a position dependent mass. They found numerical results based on Caputo and Atangana-Baleanu-Caputo fractional derivatives. Amin et al [18] investigated a fractional SIRS model for the disease HRSV using the Mittag-Leffler kernel. Amin et al [19] introduced a general form of a fractional optimal control model with singular or non-singular kernels. They compared their results found using the Mittag-Leffler kernel with those found using other fractional- and integer-order derivatives [19]. They examined the effect of treatment of HRSV based on an optimal control strategy of the evolution of susceptible, infectious and recovered individuals. Devendra et al [15] proposed an exothermic reaction model with a constant heat source in porous media with strong memory effects. They utilized the fractional Laplace decomposition technique based on the Caputo, Caputo-Fabrizio and Atangana-Baleanu fractional operators to find numerical solutions of this model based on a fractional energy balance equation. Also, Devendra et al [16] proposed and studied the behavior of SIRS-SI malaria transmission using a fractional SIRS-SI malaria model and examined a number of cures, such as the utilization of vaccines, antimalarial medicines and spraying. They used HATM and Padé approximation to perform numerical simulations. Devendra et al. [17] Devendra investigated a fractional extension of the vibration equation for very large membranes with distinct special cases in the Atangana-Baleanu sense and calculated numerical solutions using a homotopic technique. These recent advancements in numerical methods for fractional order models have shown that they can be used as very accurate tools to model the real world problems. In this direction, several recent procedures have been suggested, see [20, 21, 22].

Scott et al. studied an extension of the model of Scott [23] to model three species isothermal chemical reactions to include aperiodic responses and an isothermal response capable of supporting complex periodic reactions. This model includes three intermediate chemical species, A , B and C, for a chemical reaction which converts the relatively stable precursor reactant P to a final product D. These chemical reactions are

$$P \to U, \quad \text{rate} = k_0 p, \tag{1}$$

$$P + W \to U + W, \quad \text{rate} = k_w p w, \tag{2}$$

$$U \to V, \quad \text{rate} = k_a u, \tag{3}$$

$$U + 2V \to 3V, \quad \text{rate} = k_1 u v^2, \tag{4}$$

$$V \to W, \quad \text{rate} = k_2 V, \tag{5}$$

$$W \to D, \quad \text{rate} = k_3 w, \tag{6}$$

By applying a mass action analysis to (1)–(6), the governing rate equations based on these reactions are

$$\frac{dp}{d\tau} = -k_0 p - k_w p w, \tag{7}$$

$$\frac{du}{d\tau} = k_0 p + k_w p w - k_a u - k_1 u v^2, \tag{8}$$

$$\frac{dv}{d\tau} = k_a u + k_1 u v^2 - k_2 v, \tag{9}$$

$$\frac{dw}{d\tau} = k_a u + k_1 u v^2 - k_2 v, \tag{10}$$

In dimensionless form, these equations are

$$\frac{d\alpha_1}{dt} = -\rho \alpha_1 (\kappa + \alpha_4), \tag{11}$$

$$\frac{d\alpha_2}{dt} = \alpha_1 (\kappa + \alpha_4) - \alpha_2 \alpha_3^2 - \alpha_2, \tag{12}$$

$$\sigma \frac{d\alpha_3}{dt} = \alpha_2 \alpha_3^2 + \alpha_2 - \alpha_3, \tag{13}$$

$$\delta \frac{d\alpha_4}{dt} = \alpha_3 - \alpha_4, \tag{14}$$

where

$$\alpha_1 = \frac{k_c P}{k_3}, \quad \alpha_2 = \Big(\frac{k_1 k_u}{k_1^2}\Big)^{\frac{1}{2}} a, \quad \alpha_3 = \Big(\frac{k_1}{k_4}\Big)^{\frac{1}{2}}, \quad \alpha_4 = \Big(\frac{k_1 k_3^2}{k_4 k_2^2}\Big)^{\frac{1}{2}}$$

are the dimensionless concentrations of the four chemical species and $t = k_a \tau$ is the dimensionless time. In addition, the dimensionaless reaction rates are

$$\kappa = \Big(\frac{k_0 k_3}{k_2 k_c}\Big)\Big(\frac{k_1}{k_a}\Big)^{\frac{1}{2}}, \quad \delta = \Big(\frac{k_4}{k_3}\Big), \quad \sigma = \Big(\frac{k_a}{k_2}\Big), \quad \rho = \frac{k_w k_2}{k_3\Big(k_1 k_a\Big)^{\frac{1}{2}}}.$$

The importance and novelty of the results of the present work are, first of all, the study and determination of numerical solutions for the important chemical system of this paper and, secondly, the accuracy and efficiency of the results of this paper shown by comparing results obtained using two methods. Furthermore, the results obtained using these two methods are compared with those based on a third method proposed in [24]. Accordingly, these results could be useful to many chemical and physical researchers in order to relate these mathematical results with experimental results. As a result, as many fractional differential systems do not have exact solutions, there is a very strong motivation to try to study the behavior and accuracy of solutions of fractional equations governing chemical reactions. Hence, the present work focuses on first establishing schemes and iterative solutions for fractional equations governing chemical reactions and then detailing their accuracy.

In this section, we give some basic definitions from fractional calculus theory and properties of fractional derivatives, see, for example, [25, 26].

Definition 1. For $\nu > 0$, and $\alpha(t) \in L_1(a,b)$, with $L_1(a,b)$ the space of all integrable functions on (a,b), then the Riemann-Liouville fractional integral of order ν, denoted by J_0^ν, is given by

$$J_0^\nu \alpha(t) = \frac{1}{\Gamma(\nu)} \int_0^t (t-\eta)^{\alpha-1} \alpha(\eta) d\eta. \tag{15}$$

Definition 2. For $\nu > 0$, the Liouville-Caputo fractional derivative of order ν, denoted by ${}^{LC}D_0^\nu$, is defined by

$${}^{\mathrm{LC}}{}_0\mathcal{D}_\xi^\nu \alpha(t) = \frac{1}{\Gamma(n-\nu)} \int_0^t (t-\eta)^{n-\nu-1} \mathcal{D}^n \alpha(\eta) d\eta \tag{16}$$

$$(n-1 < \nu < n;\ n \in \mathbb{N} = \{1,2,3,\cdots\}),$$

The fractional isothermal chemical model in the Liouville-Caputo sense is obtained by replacing the derivatives $\frac{d}{dt}$ by the fractional derivatives ${}_0D_t^\nu$, $0 < \nu \leq 1$, $t > 0$, in the dimensionless chemical reaction equations (11)–(14), resulting in

$${}_0D_t^\nu \alpha_1(t) = -\rho \alpha_1(\kappa + \alpha_4), \tag{17}$$

$${}_0D_t^\nu \alpha_2(t) = \alpha_1(\kappa + \alpha_4) - \alpha_2 \alpha_3^2 - \alpha_2, \tag{18}$$

$$\sigma {}_0D_t^\nu \alpha_3(t) = \alpha_2 \alpha_3^2 + \alpha_2 - \alpha_3, \tag{19}$$

$$\delta {}_0D_t^\nu \alpha_4(t) = \alpha_3 - \alpha_4. \tag{20}$$

The main structure of the paper is as follows. In the second and third sections, the numerical scheme and solutions for the fractional isothermal chemical model in the Liouville-Caputo sense are constructed. In Section 4, the numerical results presented and investigated. Finally, in Section 5, conclusions and future research directions are presented.

2. Chebyshev spectral collocation method

Chebyshev polynomials have many applications in engineering and science. These polynomials were developed by the Russian mathematician Pafnuty Lvovich Chebyshev in 1857 [34, 35]. The main aim of this study is to implement the Chebyshev spectral collocation method (CSCM) in order to solve the FIC model given by (11)–(14) and to show that CSCM greatly simplifies this model to a non-linear system of algebraic equations which is solvable using many available numerical methods and techniques. By using well-known mathematical software, such as Mathematica or Matlab, we can easily find the Chebyshev coefficients, thereby creating numerical solutions of the fractional model presented in this paper. This is one of the advantages of CSCM, which is the ease of rapidly finding numerical solutions. This method is faster and more efficient than other methods. Among the advantages of this method are that it can be applied on finite and infinite domains and that it provides an accurate numerical technique with high efficiency and exponential rates of convergence, see [36, 40].

2.1. **Numerical Scheme and Its Convergence Analysis.** The classical orthogonal CPTK of degree n, which are orthogonal on $[-1,1]$, can be derived from the following formula (see, for example, [39] and [41])

$$P_n^{(3)}(\zeta) = \frac{\cos\big((n+\frac{1}{2})\psi\big)}{\cos\big(\frac{1}{2}\psi\big)} \qquad \big(\zeta = \cos(\psi);\ 0 \leqq \psi \leqq \pi\big).$$

In this section, we will use these functions on $[0,\hbar]$, so we construct the so-called shifted CPTK using the linear transform $\zeta = (2/\hbar)t - 1$. These shifted Chebyshev polynomials are then given by

$$\bar{\mathbb{C}}_n(t) = P_n^{(3)}\big((2/\hbar)t - 1\big),$$

where

$$\bar{\mathbb{C}}_0(t) = 1 \qquad \text{and} \qquad \bar{\mathbb{C}}_1(t) = (4/\hbar)t - 3.$$

One of the most useful formulas involving $\bar{\mathbb{C}}_n(t)$ is the analytic form given by [28, 29]

$$\bar{\mathbb{C}}_n(t) = \sum_{k=0}^{n} (-1)^k 2^{2n-2k}\, \frac{(2n+1)\Gamma(2n-k+1)}{\hbar^{n-k}\Gamma(k+1)\,\Gamma(2n-2k+2)}\, t^{n-k}, \qquad (n = 2,3,4,\cdots).$$

The function $\alpha(t) \in L_2[0,\hbar]$ can be approximated as a finite sum of $\{\bar{\mathbb{C}}_0(t), \bar{\mathbb{C}}_1(t), \cdots\}$ as

$$\alpha_m(t) = \sum_{\ell=0}^{m} a_\ell\, \bar{\mathbb{C}}_\ell(t). \tag{21}$$

Theorem 1. *Suppose that the function $\alpha(t)$ satisfies $\alpha''(t) \in L_2[0,\hbar]$ and $|\alpha''(t)| \leqq \xi$, where ξ is a constant. Then the expansion* (21) *of the shifted Chebyshev polynomials is uniformly convergent and*

$$|a_\ell| < \frac{\xi}{\ell^2}, \qquad (\ell \in 1,2,...), \tag{22}$$

see [38].

Theorem 2. *Suppose that $\alpha(t) \in C^m[0,1]$. The bound of the error on approximating the function $\alpha(t)$ by the Chebyshev polynomial expansion (21) is*

$$\|\alpha(t) - \alpha_m(t)\| \leqq \frac{\varsigma \Delta^{m+1}}{(m+1)!}\sqrt{\frac{\pi}{2}} \qquad \text{and} \qquad \varsigma = max_{t\in[0,1]}\alpha^{(m+1)}(t) \tag{23}$$
$$(\Delta = max\{t_0, t - t_0\}),$$

see [38].

In this section, we also give an approximate formula for $D^\nu \alpha_m(t)$ through the following theorem.

Theorem 3. *Suppose that the function $\alpha(t)$ is approximated in the form* (21). *Then $D^\nu\big(\alpha_m(t)\big)$ can be defined by*

$$D^\nu\big(\alpha_m(t)\big) = \sum_{i=\lceil\nu\rceil}^{m} \sum_{k=0}^{i-\lceil\nu\rceil} a_i\, \Xi_{i,k}^{(\nu)}\, t^{i-k-\nu} \qquad \text{and}$$

$$\Xi_{i,k}^{(\nu)} = \frac{(-1)^k 2^{2i-2k}(2n+1)\,(2i-k)!(i-k)!}{\hbar^{n-k}(k!)\,\Gamma(2i-2k+2)\,\Gamma(i-k+1-\nu)}, \tag{24}$$

see [27, 43].

2.2. **Construction the SCM.** We will now implement the Chebyshev spectral collocation method to solve numerically the FIC model given by (11)–(14) as follows [42, **?**]

$$\alpha_{1,m}(t) = \sum_{k=0}^{m} \alpha_{1,k}\, \bar{\mathbb{C}}_k(t), \qquad \alpha_{2,m}(t) = \sum_{k=0}^{m} \alpha_{2,k}\, \bar{\mathbb{C}}_k(t),$$
$$\alpha_{3,m}(t) = \sum_{k=0}^{m} \alpha_{3,k}\, \bar{\mathbb{C}}_k(t) \qquad \text{and} \qquad \alpha_{4,m}(t) = \sum_{k=0}^{m} \alpha_{4,k}\, \bar{\mathbb{C}}_k(t). \tag{25}$$

Substituting these expanions into the FIC Eqs. (11)–(14) and using, we obtain

$$\sum_{i=\lceil\nu\rceil}^{m} \sum_{k=0}^{i-\lceil\nu\rceil} \alpha_{1,i}\, \Xi_{i,\,k}^{(\nu)}\, t^{i-k-\nu} = -\rho \left(\sum_{k=0}^{m} \alpha_{1,i}\, \bar{\mathbb{C}}_k(t) \right) \left(\kappa + \sum_{k=0}^{m} \alpha_{4,i}\, \bar{\mathbb{C}}_k(t) \right), \tag{26}$$

$$\begin{aligned} \sum_{i=\lceil\nu\rceil}^{m} \sum_{k=0}^{i-\lceil\nu\rceil} \alpha_{2,i}\, \Xi_{i,\,k}^{(\nu)}\, t^{i-k-\nu} &= \left(\sum_{k=0}^{m} \alpha_{1,i}\, \bar{\mathbb{C}}_k(t) \right) \left(\kappa + \sum_{k=0}^{m} \alpha_{4,i}\, \bar{\mathbb{C}}_k(t) \right) \\ &\quad - \left(\sum_{k=0}^{m} \alpha_{2,i}\, \bar{\mathbb{C}}_k(t) \right) \left(\sum_{k=0}^{m} \alpha_{3,i}\, \bar{\mathbb{C}}_k(t) \right)^2 \\ &\quad - \left(\sum_{k=0}^{m} \alpha_{2,i}\, \bar{\mathbb{C}}_k(t) \right), \end{aligned} \tag{27}$$

$$\begin{aligned} \sum_{i=\lceil\nu\rceil}^{m} \sum_{k=0}^{i-\lceil\nu\rceil} \alpha_{3,i}\, \Xi_{i,\,k}^{(\nu)}\, t^{i-k-\nu} &= \left(\sum_{k=0}^{m} \alpha_{2,i}\, \bar{\mathbb{C}}_k(t) \right) \left(\sum_{k=0}^{m} \alpha_{3,i}\, \bar{\mathbb{C}}_k(t) \right)^2 \\ &\quad + \left(\sum_{k=0}^{m} \alpha_{2,k}\, \bar{\mathbb{C}}_k(t) \right) - \left(\sum_{k=0}^{m} \alpha_{3,i}\, \bar{\mathbb{C}}_k(t) \right), \end{aligned} \tag{28}$$

$$\sum_{i=\lceil\nu\rceil}^{m} \sum_{k=0}^{i-\lceil\nu\rceil} \alpha_{4,i}\, \Xi_{i,\,k}^{(\nu)}\, t^{i-k-\nu} = \left(\sum_{k=0}^{m} \alpha_{3,k}\, \bar{\mathbb{C}}_k(t) \right) - \left(\sum_{k=0}^{m} \alpha_{4,i}\, \bar{\mathbb{C}}_k(t) \right). \tag{29}$$

These last equations (26)–(29) will be collocated at m nodes t_p, $p = 0, 1, \ldots, m-1$, as follows

$$\sum_{i=\lceil\nu\rceil}^{m} \sum_{k=0}^{i-\lceil\nu\rceil} \alpha_{1,i}\, \Xi_{i,\,k}^{(\nu)}\, t_p^{i-k-\nu} = -\rho \left(\sum_{k=0}^{m} \alpha_{1,i}\, \bar{\mathbb{C}}_k(t_p) \right) \left(\kappa + \sum_{k=0}^{m} \alpha_{4,i}\, \bar{\mathbb{C}}_k(t_p) \right), \tag{30}$$

$$\sum_{i=\lceil\nu\rceil}^{m}\sum_{k=0}^{i-\lceil\nu\rceil}\alpha_{2,i}\,\Xi_{i,\,k}^{(\nu)}\,t_p^{i-k-\nu}=\left(\sum_{k=0}^{m}\alpha_{1,i}\,\bar{\mathbb{C}}_k(t_p)\right)\left(\kappa+\sum_{k=0}^{m}\alpha_{4,i}\,\bar{\mathbb{C}}_k(t_p)\right)-\left(\sum_{k=0}^{m}\alpha_{2,i}\,\bar{\mathbb{C}}_k(t_p)\right)\left(\sum_{k=0}^{m}\alpha_{3,i}\,\bar{\mathbb{C}}_k(t_p)\right)^2-\left(\sum_{k=0}^{m}\alpha_{2,i}\,\bar{\mathbb{C}}_k(t_p)\right),\tag{31}$$

$$\sum_{i=\lceil\nu\rceil}^{m}\sum_{k=0}^{i-\lceil\nu\rceil}\alpha_{3,i}\,\Xi_{i,\,k}^{(\nu)}\,t_p^{i-k-\nu}=\left(\sum_{k=0}^{m}\alpha_{2,i}\,\bar{\mathbb{C}}_k(t_p)\right)\left(\sum_{k=0}^{m}\alpha_{3,i}\,\bar{\mathbb{C}}_k(t_p)\right)^2+\left(\sum_{k=0}^{m}\alpha_{2,k}\,\bar{\mathbb{C}}_k(t_p)\right)-\left(\sum_{k=0}^{m}\alpha_{3,i}\,\bar{\mathbb{C}}_k(t_p)\right),\tag{32}$$

$$\sum_{i=\lceil\nu\rceil}^{m}\sum_{k=0}^{i-\lceil\nu\rceil}\alpha_{4,i}\,\Xi_{i,\,k}^{(\nu)}\,t_p^{i-k-\nu}=\left(\sum_{k=0}^{m}\alpha_{3,k}\,\bar{\mathbb{C}}_k(t_p)\right)-\left(\sum_{k=0}^{m}\alpha_{4,i}\,\bar{\mathbb{C}}_k(t_p)\right).\tag{33}$$

In addition, the associated initial conditions can be obtained by using the expansions Eqs. (25). We thus have

$$\sum_{i=0}^{m}(-1)^i(2i+1)\,\alpha_{1,i}=\alpha_{1,0},\tag{34}$$

$$\sum_{i=0}^{m}(-1)^i(2i+1)\,\alpha_{2,i}=\alpha_{2,0},\tag{35}$$

$$\sum_{i=0}^{m}(-1)^i(2i+1)\,\alpha_{3,i}=\alpha_{3,0},\tag{36}$$

$$\sum_{i=0}^{m}(-1)^i(2i+1)\,\alpha_{4,i}=\alpha_{4,0}.\tag{37}$$

Finally, Eqs. (30)–(33), together with the initial conditions (34)–(37), give rise to a non-linear system of $4(m+1)$ algebraic equations. This system of algebraic equations will be solved for the following unknowns $\alpha_{1,i}$, $\alpha_{2,i}$, $\alpha_{3,i}$, $\alpha_{4,i}$, $i=0,1,\cdots,m$, by using the Newton-Raphson iteration method.

3. Lagrange polynomial interpolation

In this section we construct the iteration formula for the solution of the fractional model using the method of [44]. This method is based on the fundamental theorem of fractional calculus and Lagrange polynomial interpolation. For this iterative formula

we apply the fundamental theorem of fractional calculus on (17)–(20) and obtain

$$\alpha_1(t)-\alpha_1(0)=\frac{1}{\Gamma(\nu)}\int_0^t\Big(-\rho\,\alpha_1(\eta)(\kappa+\alpha_4(\eta))\Big)(t-\eta)^{\nu-1}d\eta, \tag{38}$$

$$\alpha_2(t)-\alpha_2(0)=\frac{1}{\Gamma(\nu)}\int_0^t\Big(\alpha_1(\eta)(\kappa+\alpha_4(\eta))-\alpha_2(\eta)\alpha_3^2(\eta)-\alpha_2(\eta)\Big)(t-\eta)^{\nu-1}d\eta, \tag{39}$$

$$\alpha_3(t)-\alpha_3(0)=\frac{1}{\Gamma(\nu)}\int_0^t\Big(\alpha_2(\eta)\alpha_3^2(\eta)+\alpha_2(\eta)-\alpha_3(\eta)\Big)(t-\eta)^{\nu-1}d\eta, \tag{40}$$

$$\alpha_4(t)-\alpha_4(0)=\frac{1}{\Gamma(\nu)}\int_0^t\Big(\alpha_3(\eta)-\alpha_4(\eta)\Big)(t-\eta)^{\nu-1}d\eta. \tag{41}$$

These equations (38)–(41) can be reformulated as

$$\alpha_1(t_{n+1})-\alpha_1(0)=\frac{1}{\Gamma(\nu)}\sum_{m=0}^{\infty}\int_{t_m}^{t_{m+1}}\Big(-\rho\,\alpha_1(\eta)(\kappa+\alpha_4(\eta))\Big)(t_{m+1}-\eta)^{\nu-1}d\eta, \tag{42}$$

$$\begin{aligned}\alpha_2(t_{n+1})-\alpha_2(0)=&\frac{1}{\Gamma(\nu)}\sum_{m=0}^{\infty}\int_{t_m}^{t_{m+1}}\Big(\alpha_1(\eta)(\kappa+\alpha_4(\eta))-\alpha_2(\eta)\alpha_3^2(\eta)-\alpha_2(\eta)\Big)\\&\times(t_{m+1}-\eta)^{\nu-1}d\eta,\end{aligned} \tag{43}$$

$$\alpha_3(t_{n+1})-\alpha_3(0)=\frac{1}{\Gamma(\nu)}\sum_{m=0}^{\infty}\int_{t_m}^{t_{m+1}}\Big(\alpha_2(\eta)\alpha_3^2(\eta)+\alpha_2(\eta)-\alpha_3(\eta)\Big)(t_{m+1}-\eta)^{\nu-1}d\eta, \tag{44}$$

$$\alpha_4(t_{n+1})-\alpha_4(0)=\frac{1}{\Gamma(\nu)}\sum_{m=0}^{\infty}\int_{t_m}^{t_{m+1}}\Big(\alpha_3(\eta)-\alpha_4(\eta)\Big)(t_{m+1}-\eta)^{\nu-1}d\eta. \tag{45}$$

Using two step Lagrange polynomial interpolation we obtain

$$\begin{aligned}\alpha_1(t_{n+1}) &= \alpha_1(0)+\frac{1}{h\Gamma(\nu)}\sum_{m=0}^{n}\Bigg(\Big(-\rho\,\alpha_1(t_m)(\kappa+\alpha_4(t_m)\Big)\int_{t_m}^{t_{m+1}}\frac{(\eta-t_{m-1})}{(t_{m+1}-\eta)^{1-\alpha}}d\eta\\&- \Big(-\rho\,\alpha_1(t_{m-1})(\kappa+\alpha_4(t_{m-1}))\Big)\int_{t_m}^{t_{m+1}}\frac{(\eta-t_m)}{(t_{m+1}-\eta)^{1-\nu}}d\eta\Bigg)\end{aligned}$$

$$\begin{aligned}\alpha_2(t_{n+1}) &= \alpha_2(0)+\frac{1}{h\Gamma(\nu)}\sum_{m=0}^{n}\Bigg(\Big(\alpha_1(t_m)(\kappa+\alpha_4(t_m))-\alpha_2(t_m)\alpha_3^2(t_m)-\alpha_2(t_m)\Big)\\&\times\int_{t_m}^{t_{m+1}}\frac{(\eta-t_{m-1})}{(t_{m+1}-\eta)^{1-\nu}}d\eta-\Big(\alpha_1(t_{m-1})(\kappa+\alpha_4(t_{m-1}))\\&-\alpha_2(t_{m-1})\alpha_3^2(t_{m-1})-\alpha_2(t_{m-1})\Big)\int_{t_m}^{t_{m+1}}\frac{(\eta-t_m)}{(t_{m+1}-\eta)^{1-\nu}}d\eta\Bigg),\end{aligned} \tag{46}$$

$$\alpha_3(t_{n+1}) = \alpha_3(0) + \frac{1}{h\Gamma(\nu)} \sum_{m=0}^{n} \Bigg(\Big(\alpha_2(t_m)\alpha_3^2(t_m) + \alpha_2(t_m) - \alpha_3(t_m) \Big) \times \int_{t_m}^{t_{m+1}} \frac{(\eta - t_{m-1})}{(t_{m+1} - \eta)^{1-\nu}} d\eta - \Big(\alpha_2(t_{m-1})\alpha_3^2(t_{m-1}) + \alpha_2(t_{m-1}) - \alpha_3(t_{m-1}) \Big) \int_{t_m}^{t_{m+1}} \frac{(\eta - t_m)}{(t_{m+1} - \eta)^{1-\nu}} d\eta \Bigg), \tag{47}$$

$$\alpha_4(t_{n+1}) = \alpha_4(0) + \frac{1}{h\Gamma(\nu)} \sum_{m=0}^{n} \Bigg(\Big(\alpha_3(t_m) - \alpha_4(t_m) \Big) \int_{t_m}^{t_{m+1}} \frac{(\eta - t_{m-1})}{(t_{m+1} - \eta)^{1-\nu}} d\eta - \Big(\alpha_3(t_{m-1}) - \alpha_4(t_{m-1}) \Big) \int_{t_m}^{t_{m+1}} \frac{(\eta - t_m)}{(t_{m+1} - \eta)^{1-\nu}} d\eta \Bigg). \tag{48}$$

The integrals in these Lagrange interpolation formulae are evaluated directly. The numerical solution of (17)–(20) involving the LC derivative is then given by

$$\alpha_1(t_{n+1}) = \alpha_1(0) + \frac{h^\nu}{\nu(1+\nu)\Gamma(\nu)} \sum_{m=0}^{n} \Bigg(\Big(- \rho\, \alpha_1(t_m)(\kappa + \alpha_4(t_m)) \Big) \Theta_1(n,m) - \Big(- \rho\, \alpha_1(t_{m-1})(\kappa + \alpha_4(t_{m-1})) \Big) \Theta_2(n,m) \Bigg), \tag{49}$$

$$\alpha_2(t_{n+1}) = \alpha_2(0) + \frac{h^\nu}{\nu(1+\nu)\Gamma(\nu)} \sum_{m=0}^{n} \Bigg(\Big(\alpha_1(t_m)(\kappa + \alpha_4(t_m)) - \alpha_2(t_m)\alpha_3^2(t_m) - \alpha_2(t_m) \Big) \times \Theta_1(n,m) - \Big(\alpha_1(t_{m-1})(\kappa + \alpha_4(t_{m-1})) - \alpha_2(t_{m-1})\alpha_3^2(t_{m-1}) - \alpha_2(t_{m-1}) \Big) \Theta_2(n,m) \Bigg), \tag{50}$$

$$\alpha_3(t_{n+1}) = \alpha_3(0) + \frac{h^\nu}{\nu(1+\nu)\Gamma(\nu)} \sum_{m=0}^{n} \Bigg(\Big(\alpha_2(t_m)\alpha_3^2(t_m) + \alpha_2(t_m) - \alpha_3(t_m) \Big) \times \Theta_1(n,m) - \Big(\alpha_2(t_{m-1})\alpha_3^2(t_{m-1}) + \alpha_2(t_{m-1}) - \alpha_3(t_{m-1}) \Big) \Theta_2(n,m) \Bigg), \tag{51}$$

$$\alpha_4(t_{n+1}) = \alpha_4(0) + \frac{h^\nu}{\nu(1+\nu)\Gamma(\nu)} \sum_{m=0}^{n} \Bigg(\Big(\alpha_3(t_m) - \alpha_4(t_m) \Big) \Theta_1(n,m) - \Big(\alpha_3(t_{m-1}) - \alpha_4(t_{m-1}) \Big) \Theta_2(n,m) \Bigg). \tag{52}$$

$$\Theta(n,m) = \Big((n+1-m)^\nu (n-m+2+\nu) - (n-m)^\nu \times (n-m+2+2\nu) \Big), \tag{53}$$

$$\Theta_2(n,m) = \Big((n+1-m)^{\nu+1} - (n-m)^{\nu}(n-m+1+\nu)\Big). \tag{54}$$

4. Numerical Results and Discussion

In this section we discuss numerical results obtained using methods presented in the previous sections. We plot the numerical solutions for both methods for different values of ν. In Figure 1, the two numerical solutions are shown for $\nu = 1$, $m = 21$, $h = 0.003$, $L = 10$, $\rho = 0.5$, $\kappa = 0.1$, $\sigma = 0.05$ and $\delta = 2$. From this figure it is clear that the two solutions are in agreement, both in terms of the overall behavior and the detailed agreement. In Figure 2, the absolute errors between the two solutions for the same parameter values as Figure 1 are shown. It is clear that from this figure that the error is very small and that the error between the two solutions decreases as more terms are used in the SCM and more iterates are used in the LP method. In Figure 3, the two numerical solutions for SCM and LPI are also compared, but in this case for non-integer ν and the parameter values $\nu = 0.7$, $m = 21$, $h = 0.003$, $L = 30$, $\rho = 0.05$, $\kappa = 2$, $\sigma = 0.05$ and $\delta = 0.2$. This comparison is key, as most previous work has not considered non-integer ν. It is also clear from this figure that there is good agreement between the two solutions. In Figure 4, the absolute error between the two numerical solutions is shown. It is clear that the error is small and decreases as the number of terms in the SCM increases and as the number of iterations in the LPI increases. Through these figures and the associated results we see the accuracy and effectiveness of the two methods. We can then conclude that these methods can be used to solve fractional models for which exact solutions are difficult, or impossible, to obtain. To verify the accuracy of the methods of this paper in the non-integer case we shall now compare results obtained using them with solutions obtained using the four stage fractional Runge-Kutta method (FSFRK). These comparisons are shown in Tables 1 to 4. From these tables, we note that the absolute error between with the two methods of this paper is very small and is of the order 10^{-4}–10^{-6}, while the absolute error between the two methods separately with the FSFRK is of the order 10^{-1}–10^{-2}. We note that there is no exact solution in the fractional case to compare with. However, we can conclude that the FSFRK is better than the two methods of this paper in the integer case, while in the non-integer case, the two methods of this work are better. Finally, as a general conclusion from the figures of this paper, we can confirm the efficiency of the present algorithm and its computationally favorable use for the numerical treatment of the chemical reaction model.

n	$\lvert\alpha_{1,SCM}(t)-\alpha_{1,LPI}(t)\rvert$	$\lvert\alpha_{1,SCM}(t)-\alpha_{1}(t)\rvert$[24]	$\lvert\alpha_{1,LPI}(t)-\alpha_{1}(t)\rvert$[24]
0	2.60208×10^{-18}	0.	2.60209×10^{-18}
200	6.02204×10^{-5}	2.99953×10^{-2}	2.99351×10^{-2}
400	1.16289×10^{-5}	3.24614×10^{-2}	3.24497×10^{-2}
600	1.45956×10^{-5}	3.00798×10^{-2}	3.00652×10^{-2}
800	1.07694×10^{-5}	2.72211×10^{-2}	2.72103×10^{-2}
1000	4.71929×10^{-6}	2.48346×10^{-2}	2.48298×10^{-2}
1200	4.47128×10^{-6}	2.30074×10^{-2}	2.30029×10^{-2}
1400	3.86194×10^{-6}	2.16387×10^{-2}	2.16348×10^{-2}
1600	2.04109×10^{-7}	2.06152×10^{-2}	2.06149×10^{-2}
1800	3.65703×10^{-6}	1.98468×10^{-2}	1.98431×10^{-2}
2000	1.31879×10^{-6}	1.9268×10^{-2}	1.92693×10^{-2}
2200	2.43018×10^{-6}	1.88317×10^{-2}	1.88292×10^{-2}
2400	8.42236×10^{-7}	1.85039×10^{-2}	1.85048×10^{-2}
2600	1.14618×10^{-7}	1.82601×10^{-2}	1.826×10^{-2}
2800	8.56490×10^{-7}	1.8082×10^{-2}	1.80829×10^{-2}
3000	8.07654×10^{-6}	1.79559×10^{-2}	1.7964×10^{-2}

TABLE 1. **Absolute error between the numerical solutions $\alpha_1(t)$ via different methods with the parameters** $\nu=0.8, m=21, h=0.003, L=10, \rho=0.5, \kappa=0.001, \sigma=0.05, \delta=1$.

n	$\lvert\alpha_{1,SCM}(t)-\alpha_{2,LPI}(t)\rvert$	$\lvert\alpha_{2,SCM}(t)-\alpha_{2}(t)\rvert$[24]	$\lvert\alpha_{2,LPI}(t)-\alpha_{2}(t)\rvert$[24]
0	6.07153×10^{-18}	0.	6.07153×10^{-18}
200	4.92884×10^{-5}	4.08968×10^{-2}	4.08475×10^{-2}
400	5.69901×10^{-5}	5.43755×10^{-2}	5.43185×10^{-2}
600	4.03982×10^{-5}	5.00733×10^{-2}	5.00329×10^{-2}
800	2.19229×10^{-5}	4.28086×10^{-2}	4.27867×10^{-2}
1000	2.42961×10^{-5}	3.61967×10^{-2}	3.61724×10^{-2}
1200	1.26664×10^{-5}	3.08192×10^{-2}	3.08065×10^{-2}
1400	1.2939×10^{-5}	2.6552×10^{-2}	2.65391×10^{-2}
1600	1.00215×10^{-5}	2.31606×10^{-2}	2.31505×10^{-2}
1800	5.99963×10^{-6}	2.04379×10^{-2}	2.04319×10^{-2}
2000	8.28771×10^{-6}	1.82249×10^{-2}	1.82166×10^{-2}
2200	3.28531×10^{-6}	1.64038×10^{-2}	1.64005×10^{-2}
2400	5.35059×10^{-6}	1.48873×10^{-2}	1.4882×10^{-2}
2600	3.93416×10^{-6}	1.36108×10^{-2}	1.36069×10^{-2}
2800	4.77267×10^{-6}	1.25254×10^{-2}	1.25206×10^{-2}
3000	1.19682×10^{-5}	1.15941×10^{-2}	1.15821×10^{-2}

TABLE 2. **Absolute error between the numerical solutions $\alpha_2(t)$ via different methods with the parameters** $\nu=0.8, m=21, h=0.003, L=10, \rho=0.5, \kappa=0.001, \sigma=0.05, \delta=1$.

n	$\lvert\alpha_{3,SCM}(t)-\alpha_{3,LPI}(t)\rvert$	$\lvert\alpha_{3,SCM}(t)-\alpha_{3}(t)\rvert$[24]	$\lvert\alpha_{3,LPI}(t)-\alpha_{3}(t)\rvert$[24]
0	1.04083×10^{-17}	0.	1.04083×10^{-17}
200	2.45785×10^{-5}	3.06282×10^{-2}	3.06036×10^{-2}
400	5.30771×10^{-5}	5.85204×10^{-2}	5.84673×10^{-2}
600	3.66593×10^{-5}	5.87576×10^{-2}	5.87209×10^{-2}
800	3.11229×10^{-5}	5.18448×10^{-2}	5.18136×10^{-2}
1000	2.33345×10^{-5}	4.4461×10^{-2}	4.44376×10^{-2}
1200	1.98171×10^{-5}	3.81169×10^{-2}	3.80971×10^{-2}
1400	1.31221×10^{-5}	3.29483×10^{-2}	3.29352×10^{-2}
1600	1.37472×10^{-5}	2.87791×10^{-2}	2.87654×10^{-2}
1800	7.69093×10^{-6}	2.54017×10^{-2}	2.53941×10^{-2}
2000	9.47462×10^{-6}	2.26409×10^{-2}	2.26315×10^{-2}
2200	5.19805×10^{-6}	2.03606×10^{-2}	2.03554×10^{-2}
2400	6.45289×10^{-6}	1.84576×10^{-2}	1.84511×10^{-2}
2600	3.96895×10^{-6}	1.68534×10^{-2}	1.68494×10^{-2}
2800	3.41791×10^{-6}	1.54886×10^{-2}	1.54852×10^{-2}
3000	5.51117×10^{-6}	1.43173×10^{-2}	1.43118×10^{-2}

TABLE 3. **Absolute error between the numerical solutions $\alpha_3(t)$ via different methods with the parameters $\nu=0.8, m=21, h=0.003, L=10, \rho=0.5, \kappa=0.001, \sigma=0.05, \delta=1$.**

n	$\lvert\alpha_{4,SCM}(t)-\alpha_{4,LPI}(t)\rvert$	$\lvert\alpha_{4,SCM}(t)-\alpha_{4}(t)\rvert$[24]	$\lvert\alpha_{4,LPI}(t)-\alpha_{4}(t)\rvert$[24]
0	2.77556×10^{-17}	0.	2.77556×10^{-17}
200	5.32337×10^{-4}	1.8888×10^{-1}	1.88348×10^{-1}
400	1.20797×10^{-4}	2.00223×10^{-1}	2.00102×10^{-1}
600	1.32488×10^{-4}	1.78051×10^{-1}	1.77919×10^{-1}
800	1.15042×10^{-4}	1.5151×10^{-1}	1.51395×10^{-1}
1000	5.08749×10^{-5}	1.28395×10^{-1}	1.28344×10^{-1}
1200	5.98567×10^{-5}	1.09807×10^{-1}	1.09747×10^{-1}
1400	4.45511×10^{-5}	9.50965×10^{-2}	9.50519×10^{-2}
1600	1.92651×10^{-5}	8.3395×10^{-2}	8.33758×10^{-2}
1800	4.46373×10^{-5}	7.39762×10^{-2}	7.39316×10^{-2}
2000	2.07441×10^{-6}	6.62934×10^{-2}	6.62914×10^{-2}
2200	3.44291×10^{-5}	5.99455×10^{-2}	5.9911×10^{-2}
2400	4.81463×10^{-6}	5.46374×10^{-2}	5.46326×10^{-2}
2600	1.39483×10^{-5}	5.01503×10^{-2}	5.01364×10^{-2}
2800	3.34797×10^{-6}	4.63193×10^{-2}	4.63159×10^{-2}
3000	5.81874×10^{-5}	4.30186×10^{-2}	0.04308×10^{-2}

TABLE 4. **Absolute error between the numerical solutions $\alpha_4(t)$ via different methods with the parameters $\nu=0.8, m=21, h=0.003, L=10, \rho=0.5, \kappa=0.001, \sigma=0.05, \delta=1$.**

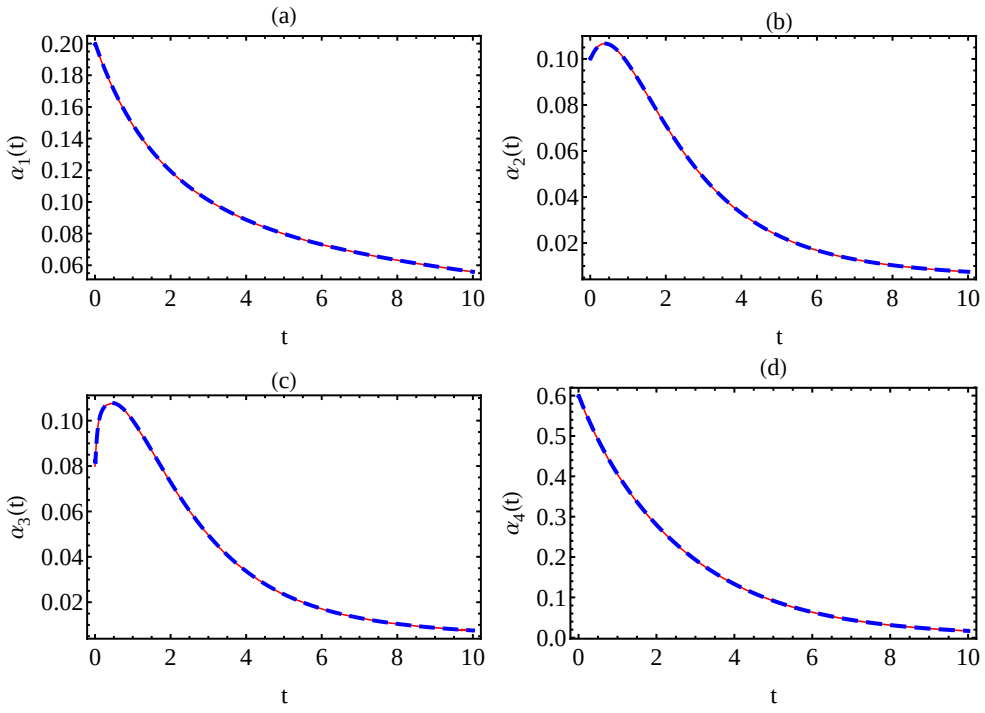

FIGURE 1. **Comparison between the numerical solutions for $\nu = 1, m = 21, h = 0.003, L = 10, \rho = 0.5, \kappa = 0.1, \sigma = 0.05, \delta = 2$. (Red solid color: SCM; Blue dashed color: LPI)**

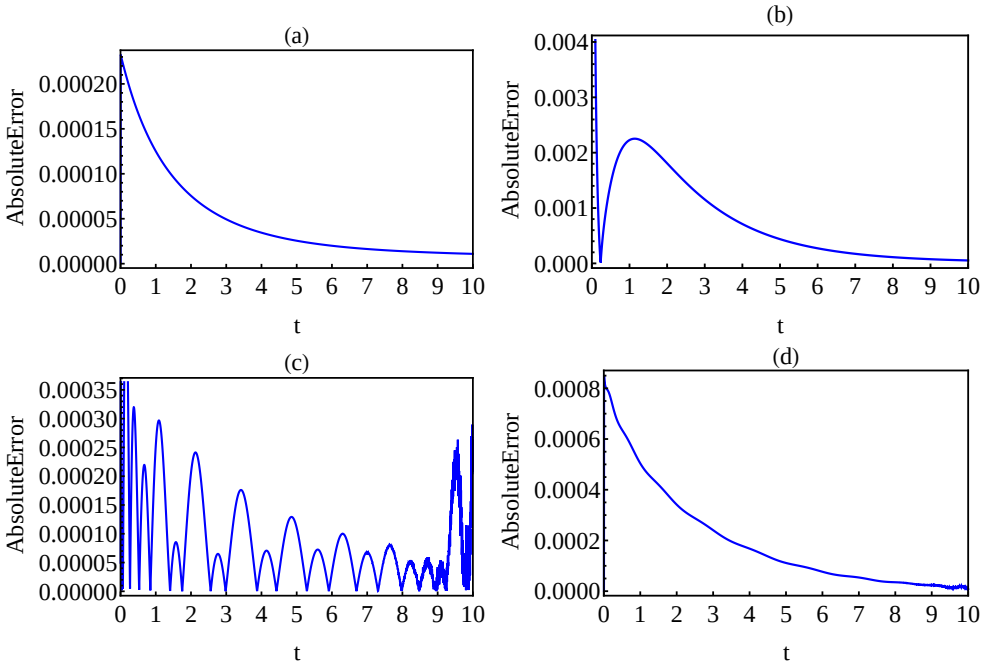

FIGURE 2. **The absolute error between the numerical solutions for $\nu = 1, m = 21, h = 0.003, L = 10, \rho = 0.5, \kappa = 0.1, \sigma = 0.05, \delta = 2$.**

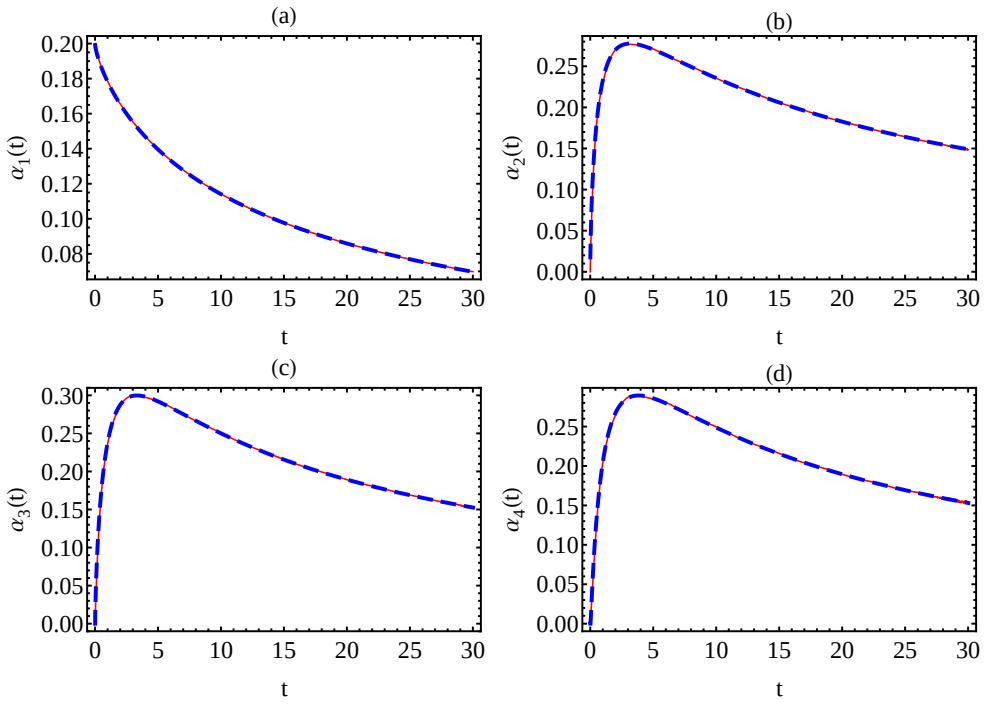

FIGURE 3. **Comparison between the numerical solutions for $\nu = 0.7, m = 21, h = 0.003, L = 30, \rho = 0.05, \kappa = 2, \sigma = 0.05, \delta = 0.2$. (Red solid color: SCM; Blue dashed color: LPI)**

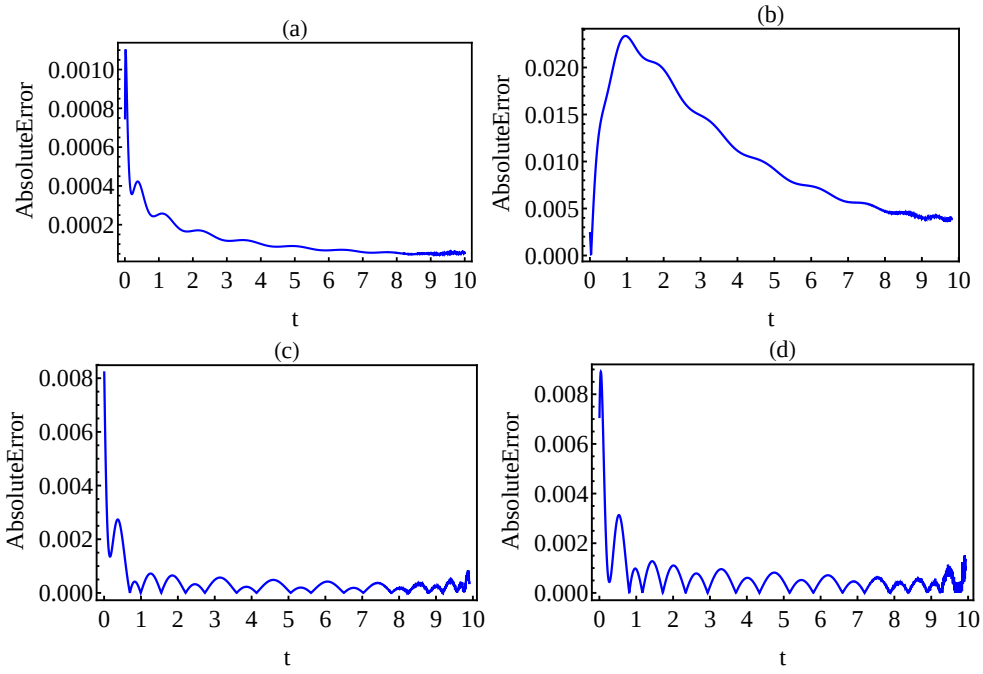

FIGURE 4. **The absolute error between the numerical solutions for** $\nu = 0.7, m = 21, h = 0.003, L = 30, \rho = 0.05, \kappa = 2, \sigma = 0.05, \delta = 0.2$**.**

5. Conclusion

In this paper, we have presented two numerical methods for calculating numerical solutions for the FIC model arising in chemical reaction theory. The SCM scheme relies on the use of Chebyshev polynomials of the third kind. The LPI method was based on iterative formulas founded on the fundamental theorem of fractional calculus. The numerical solutions obtained using these two methods were compared, with the absolute error between them calculated. It was found that there was good agreement, with the absolute error decreasing as the number of terms in the SCM increases and as the number of iterations of the LPI increases. Hence, the two methods can be used to find numerical solutions of fractional models, which usually have no exact solutions. As future work, we will extend the use of these numerical methods to find solutions of models of physical processes with space-time fractional derivatives and governed by fractional integral equations. In addition, the methods will be used to find numerical solutions of equations with other fractional operators, an example being fractional operators involving exponential and Mittag-Leffler kernels.

6. Acknowledgments

The author thanks Noel F. Smyth, University of Edinburgh for reading and editing this manuscript.

Conflicts of Interest: The author declares that he has no conflicts of interest.

References

[1] R. Caponetto and G. Dongola and L. Fortuna and I. PetráS, Fractional order systems: modeling and control applications,World Scientific, 2010

[2] M. A. Concepción, Y. ChenBlas, B. M. Vinagre, X. VinagreDingyü, F. Vicente, Fractional-order Systems and Controls , Springer, London, 2010 ,doi.org/10.1007/978-1-84996-335-0.

[3] S.-J. Liao. On the homotopy analysis method for nonlinear problems. Appl. Math. Comput. 147(2004) 499–513.

[4] K. M. Saad, E. H. F AL-Shareef, A. K. Alomari, D. Baleanu, J. F. Gmez-Aguilar, On exact solutions for timefractional Korteweg-de Vries and Korteweg-de Vries-Burgers equations using homotopy analysis transform method, Chinese Journal of Physics 63(2020) 149–162.

[5] J. H. He, Variational iteration method-a kind of nonlinear analytical technique: some examples. Int. J. Non-Linear Mech. 34(1999) 708–799.

[6] K. M. Saad, E. H. F Al-Sharif Analytical study for time and time-space fractional Burgers equation Advances in Difference Equations 2017 (1)(2017) 300.

[7] X. C. Shi, L. L. Huang, Y. Zeng, Fast Adomian decomposition method for the Cauchy problem of the time-fractional reaction diffusion equation. Adv. Mech. Eng. 8(2), 1-5 (2016)

[8] H. M. Srivastava, K. M. Saad , New approximate solution of the time-fractional Nagumo equation involving fractional integrals without singular kernel , Appl. Math. Inf. Sci 14(1)(2020) 1–8.

[9] A. Bueno-Orovio, D. Kay, K. Burrage, Fourier spectral methods for fractional-in-space reaction-diffusion equations, Bit Numer Math 54(2014) 937–954.

[10] Y. Takeuchi, Y. Yoshimoto, R. Suda: Second order accuracy finite difference methods for space-fractional partial differential equations. J. Comput. Appl. Math. 320(2017)101-119.

[11] Y Šocel, K. Yildiray, K. Aydin: The solution of the Bagley Torvik equation with the generalized Taylor collocation method. J. Franklin Inst. 347(2)(2010) 452–466.

[12] D. Kumar, J. Singh, K. Tanwar, D. Baleanu, A new fractional exothermic reactions model having constant heat source in porous media with power, exponential and Mittag-Leffler laws, International Journal of Heat and Mass Transfer 138(2019) 1222–1227.

[13] Kumar D, Singh J, Baleanu D. On the analysis of vibration equation involving a fractional derivative with Mittag-Leffler law. Math Meth Appl Sci. 43(2020)443–457.
[14] D. Baleanu and A. Jajarmi, S. S. Sajjadi, J. H Asad, The fractional features of a harmonic oscillator with position-dependent mass. Communications in Theoretical Physics 72(5)(2020) 055002.
[15] D. Kumar, J. Singh, K. Tanwar, D. Baleanu, A new fractional exothermic reactions model having constant heat source in porous media with power, exponential and Mittag-Leffler Laws, International Journal of Heat and Mass Transfer 138 (2019), 1222-1227.
[16] D. Kumar, J. Singh, M. Al Qurashi et al. A new fractional SIRS-SI malaria disease model with application of vaccines, antimalarial drugs, and spraying. Adv Differ Equ 2019(2019), https://doi.org/10.1186/s13662-019-2199-9
[17] D. Kumar, J. Singh, D. Baleanu, On the analysis of vibration equation involving a fractional derivative with Mittag-Leffler law, Mathematical Methods in the Applied Sciences 43(1) (2019) 443–457.
[18] A. Jajarmi, A. Yusuf, D. Baleanu, M. Inc, A new fractional HRSV model and its optimal control: A non-singular operator approach, Physica A: Statistical Mechanics and its Applications Volume 547(1)(20200)123860.
[19] A. Jajarmi, D. Baleanu, On the fractional optimal control problems with a general derivative operator, Asian Journal of Control, (2019), doi.org/10.1002/asjc.2282
[20] S. Bhatter, A. Mathur, D. Kumar, J. Singh, A new analysis of fractional Drinfeld-Sokolov-Wilson model with exponential memory, Physica A 537 (2020) 122578.
[21] P. Veeresha, D. G. Prakasha, D. Kumar, D. Baleanu, J. Singh, An efficient computational technique for fractional model of generalized Hirota-Satsuma coupled KdV and coupled mKdV equations, Journal of Computational and Nonlinear Dynamics 15 (2020) 071003.
[22] A. Goswami, J. Singh, D. Kumar, Sushila, An efficient analytical approach for fractional equal width equations describing hydro-magnetic waves in cold plasma, Physica A 524(2019) 563–575.
[23] S. K. Scott, Transient chaos in a closed chemical system, J. Chem. Phys. 94 (1991) 1134, https://doi.org/10.1063/1.460019
[24] C. Milici, J. A. T. Machado and G. Drăgănescu, Application of the Euler and Runge-Kutta generalized methods for FDE and symbolic packages in the analysis of some fractional attractors, Internat. J. Nonlinear Sci. Numer. Simul. 21(2)(2020) 159–170.
[25] A. A. Kilbas, H. M. Srivastava and J. J. Trujillo, Theory and Applications of Fractional Differential Equations, North-Holland Mathematical Studies, 204, Elsevier (North-Holland) Science Publishers, Amsterdam, London and New York, 2006.
[26] I. Podlubny, Fractional Differential Equations. Academic Press, New York(1993)
[27] C. Y. Handan, Numerical solution of fractional Riccati differential equation via shifted Chebyshev polynomials of the third kind, J. Engrg. Technol. Appl. Sci. 28 (2017) 1–11.
[28] M. M. Khader, On the numerical solutions for the fractional diffusion equation, Commun. Nonlinear Sci. Numer. Simul. 16 (2011) 2535–2542.
[29] M. M. Khader and M. M. Babatin, Numerical treatment for solving fractional SIRC model and influenza A, Comput. Appl. Math. 33 (2014) 543–556.
[30] M. M. Khader, The numerical solution for BVP of the liquid film flow over an unsteady stretching sheet with thermal radiation and magnetic field using FEM, Internat. J. Modern Phys. C. 15(3)(2019)1950080.
[31] M. M. Khader and M. Adel, Introducing the windowed Fourier frames technique for obtaining the approximate solution of coupled system of differential equations, J. Pseudo-Differ. Oper. Appl. 10(2019) 241–256.
[32] M. M. Khader and M. Adel, Chebyshev wavelet procedure for solving FLDEs, Acta Appl. Math. 158(1) (2018) 1–10.
[33] M. M. Khader and K. M. Saad, Numerical treatment for studying the blood ethanol concentration systems with different forms of fractional derivatives, Internat. J. Modern Phys. C. 31(3)(2020) 2050044.
[34] P. L. Chebyshev, Théorie des mécanismes connus sous le nom de parallélogrammes, Mém. Acad. Imp. Sci. St.-Pétersbg. 7(1853)539–568.
[35] L. Fox, I. B. Parker, Chebyshev Polynomials in Numerical Analysis, Oxford University Press, LondonNew YorkToronto, 1968.

[36] M. M. Khader and K. M. Saad, A numerical study using Chebyshev collocation method for a problem of biological invasion: Fractional Fisher equation, Internat. J. Biomath 11(8)(2018) 1–15.
[37] K. M. Saad, New fractional derivative with non-singular kernel for deriving Legendre spectral collocation method, Alexandria Engineering Journal, 59(4)(2020) 1909-1917.
[38] M. M. Khader and K. M. Saad, A numerical approach for solving the problem of biological invasion (fractional Fisher equation) using Chebyshev spectral collocation method, Chaos Solitons Fractals 110(2018)169–177.
[39] J. C. Mason and D. C. Handscomb, Chebyshev Polynomials, Chapman and Hall (CRC Press), New York and Boca Raton, 2003.
[40] H. Singh and H. M. Srivastava, Jacobi collocation method for the approximate solution of some fractional-order Riccati differential equations with variable coefficients, Physica A:Statist. Mech. Appl. 523(2019)1130–1149.
[41] M. A. Snyder, Chebyshev Methods in Numerical Approximation, Prentice-Hall Incorporated, Englewood Cliffs, New Jersey, 1966.
[42] N. H. Sweilam, A. M. Nagy, A. A. El-Sayed, Second kind shifted Chebyshev polynomials for solving space fractional order diffusion equation, Chaos, Solitons & Fractals 73(2015) 141–147.
[43] N. H. Sweilam, A. M. Nagy and A. A. El-Sayed, On the numerical solution of space fractional order diffusion equation via shifted Chebyshev polynomials of the third kind, J. King Saud Univ. Sci. 28(2016) 41–47.
[44] K. M. Owolabi, A. Atangana, Numerical Simulation of Noninteger Order System in Subdiffusive, Diffusive, and Superdiffusive Scenarios, Journal of Computational and Nonlinear Dynamics. 12(3)(2017) 1–7.